Journal Publication of International Research for Engineering and Management (JOIREM)
Volume: 04 Issue: 4| April 2026
ISSN (O) 3107-6696

STSMC-BASED ANALYSIS AND ADRC DESIGN FOR AN LCC-LCC WIRELESS POWER SYSTEM

R. Sravani[1], S. Rakesh[2], C. Ramudu[3], G. Ravi Kumar[4], T. Ganesh[5]

[1,2,3,4,5] *EEE & PSCMR college*

Abstract - This project presents that Wireless Power Transfer (WPT) systems using resonant topologies, such as the LCC–LCC configuration, offer high efficiency and stable performance for applications including electric vehicles and automated systems. However, variations in coupling and load changes introduce control challenges that affect output voltage stability. This project presents the design and evaluation of an Active Disturbance Rejection Control (ADRC) strategy enhanced with a Super-Twisting Sliding Mode Controller (STSMC) for an LCC–LCC WPT system. The proposed controller aims to improve dynamic response, reduce overshoot, and enhance robustness against disturbances and parameter uncertainties. A comparison with a conventional Proportional-Integral (PI) controller is performed to assess settling time, stability, and voltage regulation under varying load conditions. The STSMC-based ADRC controller achieves faster transient response and superior steady-state voltage regulation compared to the PI controller, demonstrating its effectiveness for reliable and efficient WPT applications.

KeyWords: High-Frequency, LCC-LCC Compensation Network, Rectifier Circuit, Dc-Dc Buck Converter. Stsmc controller

1. INTRODUCTION

Wireless Power Transfer (WPT) technology facilitates the transmission of electrical energy from a power source to devices without physical contact. This innovative method effectively mitigates issues associated with traditional contact-based power collection, such as sparking, leakage, and vulnerability to environmental factors like rain, snow, and dust. WPT has been widely applied across multiple sectors, including consumer electronics, specialized power supply environments, industrial production processes, and household appliances [1], [2], [3], [4], [5], [6]. The Wireless Power Transfer (WPT) system facilitates energy transmission via a high-frequency magnetic field established between the primary and secondary sides. The coils on both sides can be modelled as loosely coupled transformers, primarily due to the low coupling coefficient resulting from the air gap. To achieve resonance and ensure proper system operation, compensation capacitors are added to both the primary and secondary sides. Traditional compensation networks [7] include series-series (SS), series-parallel (SP), parallel (PP), and parallel- series (PS). However, these traditional networks may not be suitable for certain applications, leading to the widespread adoption of higher-order compensation networks such as LCL [8], LCC-S [9], LCC-LCC [10], and others. Literature [11] proposes an enhanced compensation network based on the traditional LCL topology to improve the robustness of dynamic wireless charging systems against variations in coil coupling coefficients. In this paper, the LCC-LCC topology is selected to ensure high flexibility and anti-migration performance. The LCC-LCC compensation network has garnered significant attention recently due to its constant current characteristics and load-independent current advantages. However, this approach is sensitive to changes in system parameters, leading to variations in system output. Literature [14] introduces a closed-loop control method based on a high-speed communication module, which offers high control accuracy but suffers from poor interference resistance and low reliability. To address the issues of inadequate anti-interference capability and low reliability identified in previous literature, this paper proposes a first-order Active Disturbance Rejection Control (ADRC) [15], [16] strategy based on the Generalized State-pace Average (GSSA) method. Firstly, the dynamic characteristics of the Wireless Power Transfer (WPT) system with LCC-LCC topology are analyzed using the GSSA approach, leading to the derivation of the small-signal model of the system. Subsequently, a first-order Active Disturbance Rejection Control (ADRC) strategy is developed by analyzing the primary-side current in the Wireless Power Transfer (WPT) system. This approach indirectly controls the secondary-side voltage through regulation of the primary-side current, ensuring stable load output. Secondly, the proposed first-order Active Disturbance Rejection Control (ADRC) strategy is validated through Bode diagram analysis, which demonstrates superior performance in terms of system stability and response speed compared to the Proportional-Integral (PI) control strategy. Finally, a simulation and experimental platform is established to verify that the proposed controller achieves a load response time of approximately 1.61 ms and a voltage fluctuation of about 2 V.

2. Related works

The related works consist of academic and industry research, ranging from prototypes to commercial systems. Finally, three types of WPT technology used in UAV charging are compared and discussed, and the advantages and disadvantages of each type of WPT technology are shown. The related research showed that using WPT technology to power the UAV is a promising way to enhance the endurance of the UAV.

Journal Publication of International Research for Engineering and Management (JOIREM)
Volume: 04 Issue: 4| April 2026
ISSN (O) 3107-6696

A. SYSTEM DESCRIPTION OF INTEGRATED ON-BOARD CHARGER

ANALYSIS OF THE WIRELESS POWER TRANSFER (WPT) SYSTEM MODEL The Wireless Power Transfer (WPT) system structure based on the LCC-LCC topology is shown in FIGURE 1 [17]. In FIGURE 1, Uin represents the DC power supply on the input side. Q1 to Q4 comprise the full-bridge inverter circuit. In the LCC-LCC compensation network, L1, C1, L2, C2, Cp, Cs , Lp, and Ls form the resonant network. The bus capacitance CH, switch S, continuous diode D, filter capacitance C, filter inductance L, and load resistance R constitute the Buck circuit.

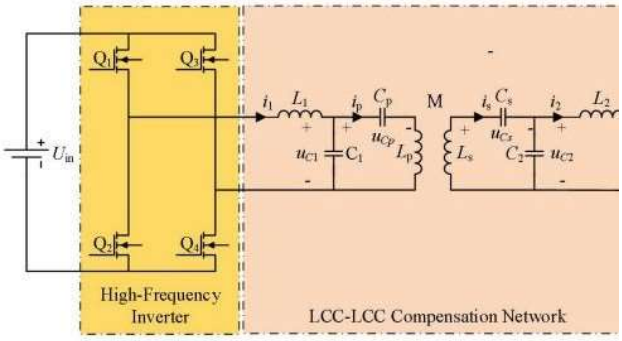

The secondary high-frequency AC is rectified to produce DC output for the Buck circuit, which is then further processed by the Buck converter before being delivered to the load side. To ensure a unity power factor in the Wireless Power Transfer (WPT) system, it is crucial to synchronize the inverter's operating frequency with the resonant frequency of the resonant network. When the LCC-LCC compensation network satisfies Equation (1), the WPT system operates at its resonant state

$$\omega = \frac{1}{\sqrt{L_1 C_1}} = \frac{1}{\sqrt{L_2 C_2}} = \frac{1}{\sqrt{(L_p - L_1)\, C_p}} = \frac{1}{\sqrt{(L_s - L_2)\, C_s}}$$

B. System Block diagram

Fig -2: System Block Diagram

B. DESIGN OF ACTIVE DISTURBANCE REJECTION CONTROL

The closed-loop control block diagram of the Wireless Power Transfer (WPT) system based on the Active Disturbance Rejection Control (ADRC) is shown in FIGURE 7

FIGURE 7. Block diagram of closed-loop control for the Wireless Power Transfer (WPT) system based on Active Disturbance Rejection Control (ADRC).

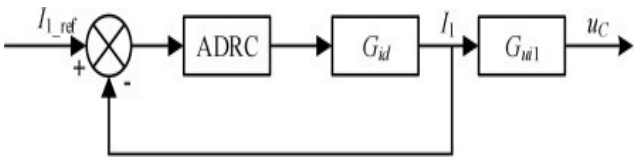

In FIGURE 7, Gid is the transfer function of the input current i1 to the duty cycle d. Gui1 is the transfer function of the secondary side voltage uC to the input current i1. The frequency response waveform of input current i1 to duty cycle d is shown in FIGURE 8. As shown in FIGURE 8, both systems incorporate an inertial link with a large time constant, providing ample response time for the closed-loop controller. The transfer function from the secondary voltage uC to the input current i1 can be derived by dividing the two transfer functions. The frequency response of the secondary-side voltage uC to the input current i1 is shown in FIGURE 9.

Software Requirements

Software Configuration:

Operating System : Windows 7/8/10

Application Software: Matlab/Simulink

Hardware Configuration:

RAM : 8 GB

Processor : I3 / I5 (Mostly prefer)

Journal Publication of International Research for Engineering and Management (JOIREM)
Volume: 04 Issue: 4| April 2026
ISSN (O) 3107-6696

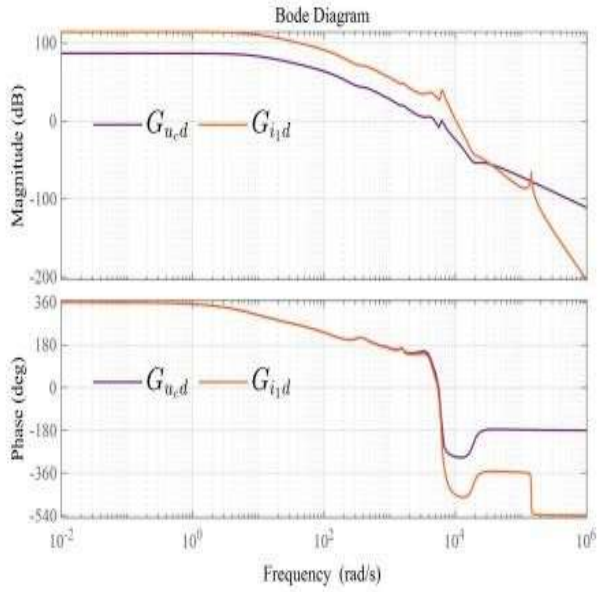

FIGURE 8. Frequency response waveform of input current i1 to duty cycle d.

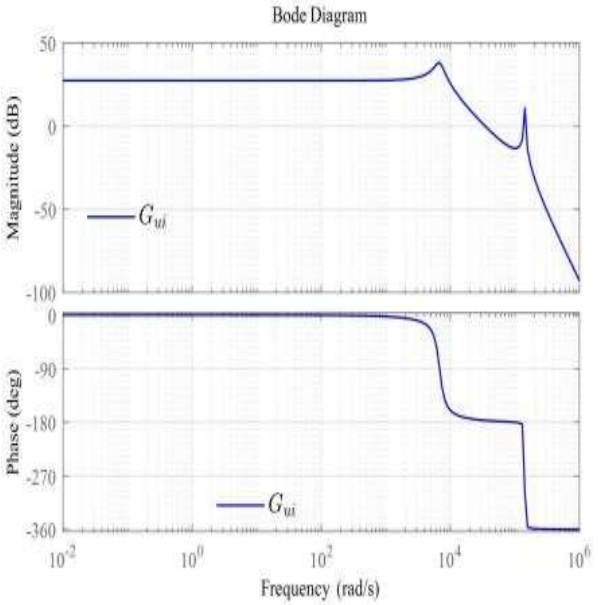

FIGURE 9. Frequency response waveform of secondary-side voltage uC to input current i1.

As shown in FIGURE 9, the input current i1 and the secondary voltage uC in the low-frequency band can be equivalent to a proportional relationship. The step response of each transfer function is shown in FIGURE 10 to more intuitively analyze the transient characteristics of input current and secondary side voltage

FIGURE 10. Step response waveforms of each system transfer function

As shown in FIGURE 10, there is a large oscillation phenomenon in the secondary side voltage uC, and the system output performance is poor. It can be seen that the reasonable design of the controller can ensure the optimal output of the system. In the control framework of Active Disturbance Rejection Control (ADRC), the expression of first-order Active Disturbance Rejection Control (ADRC) is as follows:

$$\dot{y} = f(y, u, \dot{u}) + bu \quad (20)$$

where y = I1 is the input current of the primary side; b is the gain of the Wireless Power Transfer (WPT) system; f is the total disturbance of the system; u is the system input control vector.

2. Extension results and discussion

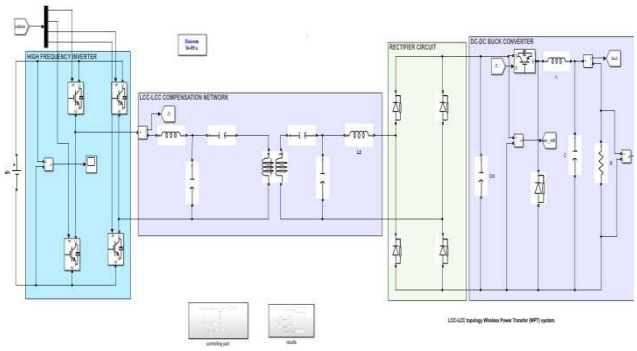

Simulation of LCC-LCC topology Wireless Power Transfer (WPT) system

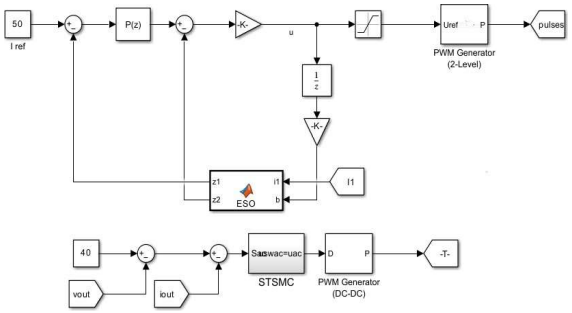

Journal Publication of International Research for Engineering and Management (JOIREM)
Volume: 04 Issue: 4| April 2026
ISSN (O) 3107-6696

CONTROLLING PART

Figure 13

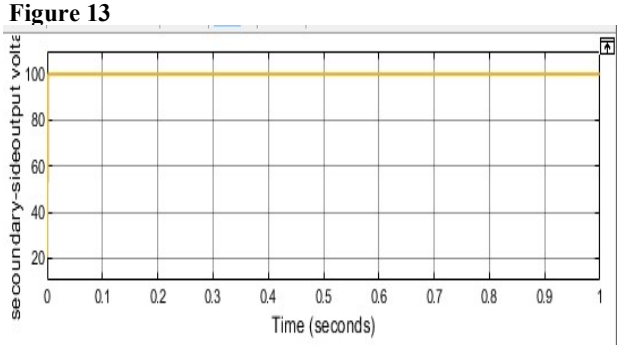

The above figure shows the simulated waveform of the secondary-side output voltage of the Wireless Power Transfer (WPT) system using Active Disturbance Rejection Control (ADRC) with the STSMC controller. This simulation evaluates the fast dynamic response and voltage regulation performance of each controller under standard operating conditions.

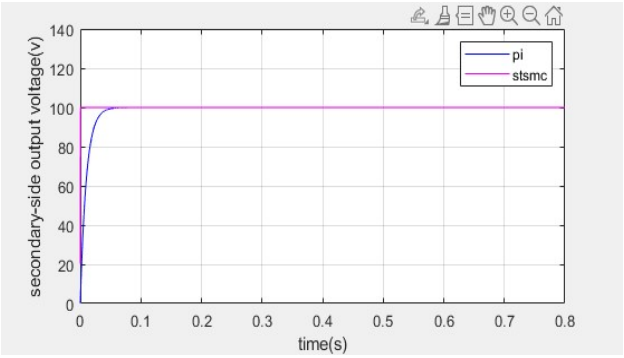

By comparing the PI and STSMC controllers, it is observed that the STSMC achieves a faster dynamic response and superior steady-state

Figure 14

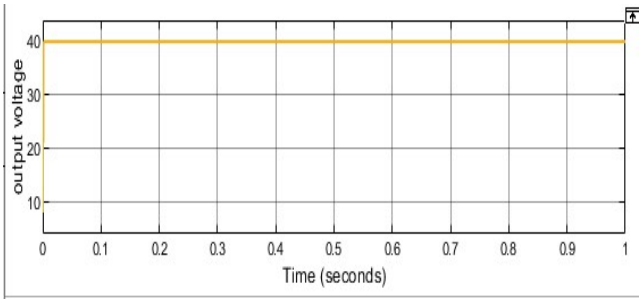

OUTPUT VOLTAGE

This figure illustrates the dynamic response of the output voltage at the load side of the Wireless Power Transfer (WPT) system under Active Disturbance Rejection Control (ADRC) with the STSMC controller. It is used to validate the controller's capability to regulate the final DC output

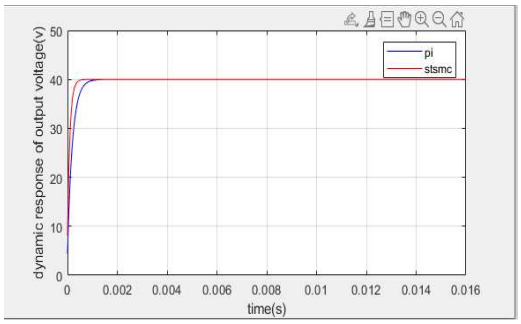

Comparison graph of both pi and stsmc controller of the output voltage

Figure 15

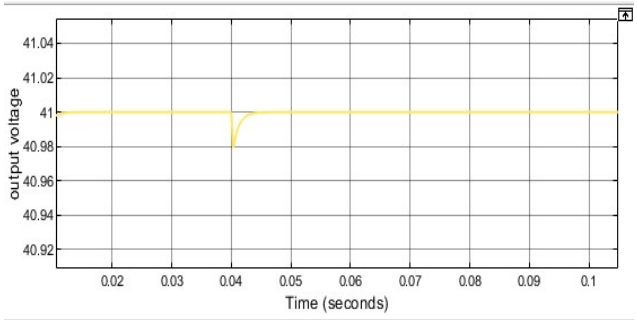

Figure 15 illustrates the dynamic output voltage response of the WPT system when the load resistance decreases from 20 Ω to 15 Ω at approximately 0.02 s using the STSMC controller. This scenario evaluates the robustness and adaptability of the control strategy under a sudden reduction in load impedance, which typically results in an increased output current and may cause a voltage dip or overshoot.

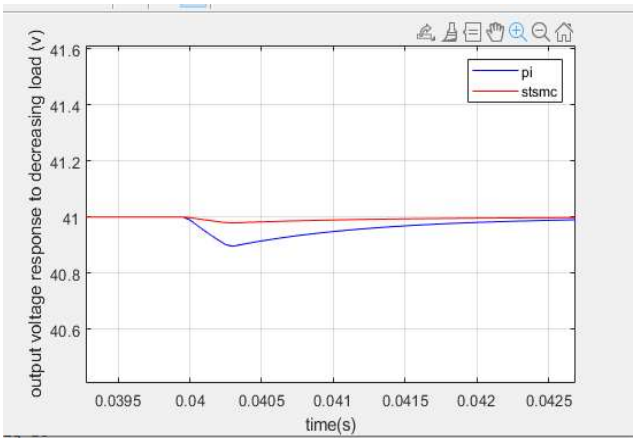

A comparison of the PI and STSMC controllers shows that the PI controller exhibits a voltage dip at around 0.04 s, whereas the STSMC controller experiences a dip earlier at approximately 0.02 s and quickly stabilizes the voltage, demonstrating faster recovery and better regulation performance

Figure 16.

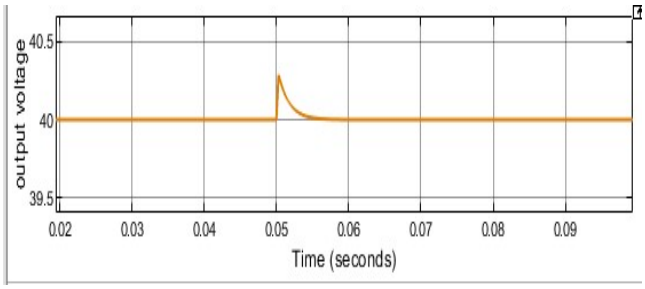

Waveform of the output voltage response to an increasing load resistance using the STSMC controller.

Table 1
Reliability of the System to Detect Faults

Corrective Action Applied On	Pass	Fail
Overvoltage	30	0
Undervoltage	30	0
Overcurrent	30	0
Undercurrent	30	0
Over Temperature	30	0

$$Reliability = \frac{Pass}{Pass + Fail} \times 100\%$$

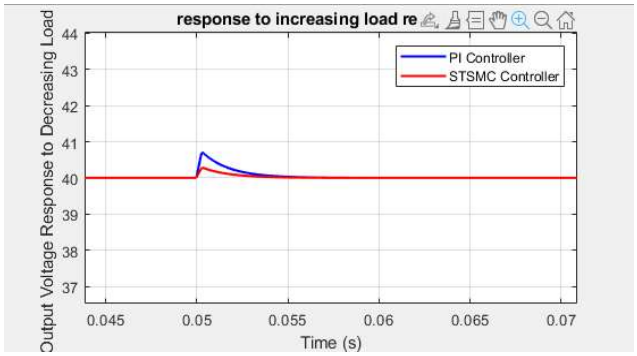

Conclusion

This project concluded that design, implementation, and analysis of an ADRC-based control strategy enhanced with a Super-Twisting Sliding Mode Controller (STSMC) for an LCC–LCC Wireless Power Transfer (WPT) system. The control approach was developed to address key challenges such as parameter variations, nonlinear dynamics, and dynamic load conditions, which typically degrade voltage regulation and system efficiency in resonant WPT applications. The results demonstrated that the proposed STSMC-based ADRC controller significantly outperforms the conventional PI controller in terms of transient response, overshoot suppression, settling time, and steady-state accuracy. The system exhibited strong robustness against disturbances and load variations, achieving faster stabilization and improved voltage regulation without chattering effects.

REFERENCES

1. S. Li and C. C. Mi, ‘‘Wireless power transfer for electric vehicle applica tions,’’ IEEE J. Emerg. Sel. Topics Power Electron., vol. 3, no. 1, pp. 4–17, Mar. 2015.
2. Z. Zhang, H. Pang, A. Georgiadis, and C. Cecati, ‘‘Wireless power transfer—An overview,’’ IEEE Trans. Ind. Electron., vol. 66, no. 2, pp. 1044–1058, Feb. 2019.
3. J. Zhou, B. Zhang, W. Xiao, D. Qiu, and Y. Chen, ‘‘Nonlinear parity time-symmetric model for constant efficiency wireless power transfer: Application to a drone-in-flight wireless charging platform,’’ IEEE Trans. Ind. Electron., vol. 66, no. 5, pp. 4097–4107, May 2019.
4. Md. A. Ullah, R. Keshavarz, M. Abolhasan, J. Lipman, K. P. Esselle, and N. Shariati, ‘‘A review on antenna technologies for ambientRFenergyharvestingandwirelesspowertransfer: Designs,chal lengesandapplications,’’ IEEE Access, vol. 10, pp. 17231–17267, 2022.
5. V. Ramakrishnan, A. D. Savio, C. Balaji, N. Rajamanickam, H. Kotb, A. Elrashidi, and W. Nureldeen, ‘‘A comprehensive review on efficiency

enhancement of wireless charging system for the electric vehicles applica tions,'' IEEE Access, vol. 12, pp. 46967–46994, 2024.
6. M. Wu, L. Su, J. Chen, X. Duan, D. Wu, Y. Cheng, and Y. Jiang, ''Development and prospect of wireless power transfer technology used to power unmanned aerial vehicle,'' Electronics, vol. 11, no. 15, Jun. 2022, Art. no. 2297.
7. W. Zhang and C. C. Mi, ''Compensation topologies of high-power wireless power transfer systems,'' IEEE Trans. Veh. Technol., vol. 65, no. 6, pp. 4768–4778, Jun. 2016, doi: 10.1109/TVT.2015.2454292
8. L. Tianren, L. Yong, and M. Ruikun, ''Modeling and control method of induced power transmission system based on LCL-S topology,'' in Chinese, Trans. China Electrotechnical Soc., vol. 33, no. 1, pp. 104–111, 2018.
9. L. Yang, S. Jiang, C. Wang, Y. Shi, M. Wang, C. Cai, and L. Zhang, ''A high-efficiency integrated LCC/S WPT system with constant current output,'' IEEE J. Emerg. Sel. Topics Power Electron., vol. 12, no. 1, pp. 341–354, Feb. 2024
10. S. Li, W. Li, J. Deng, T. D. Nguyen, and C. C. Mi, ''Adouble-sided LCC compensation network and its tuning method for wireless power transfer,'' IEEE Trans. Veh. Technol., vol. 64, no. 6, pp. 2261–2273, Jun. 2015.
11. V. Esteve, J. Jordán, E. Sanchis-Kilders, E. J. Dede, E. Maset, J. B. Ejea, and A. Ferreres, ''Comparative study of a single inverter bridge for dual frequency induction heating using Si and SiC MOSFETs,'' IEEE Trans. Ind. Electron., vol. 62, no. 3, pp. 1440–1450, Mar. 2015
12. W. Shi, J. Deng, Z. Wang, and X. Cheng, ''The start-up dynamic analysis and one cycle control-PD control combined strategy for primary side controlled wireless power transfer system,'' IEEE Access, vol. 6, pp. 14439–14450, 2018.
13. Y.Jiang,L.Wang,Y.Wang,J.Liu,M.Wu,andG.Ning,''An alysis design, and implementation of WPT system for EV's battery charging based on optimal operation frequency range,'' IEEE Trans. Power Electron., vol. 34, no. 7, pp. 6890–6905, Jul. 2019.
14. W. Zhong and S. Y. R. Hui, ''Maximum energy efficiency operation of series-series resonant wireless power transfer systems using on-off keying modulation,'' IEEE Trans. Power Electron., vol. 33, no. 4, pp. 3595–3603, Apr. 2018.
15. K. Lakomy, R. Madonski, B. Dai, J. Yang, P. Kicki, M. Ansari, and S. Li, ''Active disturbance rejection control design with suppression of sensor noise effects in application to DC–DC buck power converter,'' IEEE Trans. Ind. Electron., vol. 69, no. 1, pp. 816–824, Jan. 2022, doi: 10.1109/TIE.2021.3055187.
16. Y. Du, W. Cao, and J. She, ''Analysis and design of active disturbance rejection control with an improved extended state observer for systems with measurement noise,'' IEEE Trans. Ind. Electron., vol. 70, no. 1, pp. 855–865, Jan. 2023, doi: 10.1109/TIE.2022.3153821.
17. Z. Luo, Y. Zhao, M. Xiong, X. Wei, and H. Dai, ''A self-tuning LCC/LCC system based on switch-controlled capacitors for constant-power wireless electric vehicle charging,'' IEEE Trans. Ind. Electron., vol. 70, no. 1, pp. 709–720, Jan. 2023.
18. J. Huang, X. He, P. Huo, and R. Xu, ''A hybrid modulation strategy for LCC–LCC compensated bidirectional wireless power transfer system to achieve high efficiency in the whole operating range,'' IEEE Trans. Ind. Electron., vol. 71, no. 1, pp. 327–337, Jan. 2024.
19. H. Wenjie and T. Wen, ''Parameter tuning of linear active disturbance rejection control based on PID parameter tuning,'' in Chinese, Control Decision, vol. 36, no. 7, pp. 1592–1600, 2019.
20. Z. Rong, H. Wenjie, and T. Wen, ''Applicability and tuning of linear active disturbance rejection control,'' in Chinese, Control Theory Appl., vol. 35, no. 11, pp. 1654–1662, 2018.